Notch Effect on Fatigue Behaviour of Microalloyed Forging Steels [1]

M. BALBI, M. BONIARDI, M. GIGLIO, L. VERGANI - Dipartimento di Meccanica Politecnico di Milano, Italy

Abstract

The fatigue behaviour of a microalloyed forging steel was analysed at two hot-forging temperature levels - one at 1240°C corresponding to the ordinary heating parameters and the other at 1060°C suited to obtain a finer grain size. The resulting behaviour was then compared with a conventional hardened and tempered steel. Fatigue tests were carried out both on smooth and keyhole-type notched specimens.
The fatigue test nucleation was studied on smooth test pieces, and the resulting experimental data were then used to predict the fatigue life of notched specimens.
Contrarily to what happens with hardening and tempering steels, predictions for microalloyed steels are almost never conservative.

Riassunto

Nel presente lavoro si è studiato il comportamento a fatica di un acciaio microlegato per stampaggio a caldo (utilizzando due differenti temperature di stampaggio: una di 1240°C corrispondente agli usuali parametri di riscaldo e una di 1060°C adatta all'ottenimento di un grano cristallino più fine), confrontandolo con quello di un acciaio da bonifica temprato e rinvenuto. Sono state eseguite prove di fatica su provini cilindrici lisci e su provini intagliati di tipo keyhole. Si è studiato l'innesco della cricca a fatica in assenza di intagli ed è stata prevista la vita a fatica dei provini intagliati sulla base dei dati ottenuti su provini lisci. Contrariamente a quanto avviene per gli acciai da bonifica le previsioni non risultano conservative.

Introduction

Keywords: Microalloyed steel, fatigue, nucleation, notch

The development of microalloyed medium carbon steels, specially designed for forged piece production, was initially successful in those industrial segments, such as automotive industry, where components are mass-produced at high rate.

Great interest, in fact, was aroused by a material able to display the same mechanical strength levels as for hardened and tempered steels, with no need however for a final heat treatment. Actually, the addition of microalloy elements in the balance of the steel chemical composition and the resort to a controlled cooling, starting from the forging temperature, allows for a metallographic structure suited to achieve such performance, with the industrial advantages of a simplified operation cycle (deletion of heat treatment, removal or reduction of straightening operations likely to be requested after heat treatment), and consequent savings in production cost and energy consumption.

The only serious obstacle to a larger diffusion of industrial applications chiefly stays in the lower shock resistance of such materials as compared to conventional heat-treated steels. However, remarkable efforts are under way be several producers [1,2] to get improved results by varying both the microalloy elements and analysis proportioning, and tuning up the cooling cycle as well.

There are several factors tied to the physical metallurgy which, through an accurate and calibrated balance of individual effects and mutual actions, concur to regulate the mechanical behaviour of such steels. Among them, one can see: strengthening by solid solution, precipitation hardening, pearlite morphology and associated lamellar spacing, ferrite/pearlite proportioning, grain size coarsening or refining, shift to solution and carbide and nitride precipitation, behaviour of complex carbo-nitrides when simultaneous additions are made of different microalloy elements.

The inherently lower toughness of ferritic-pearlitic structures in microalloyed steels as compared to the tempering martensite structures of hardening and tempering steels has drawn attention to those behaviour aspects wich are linked to crack nucleation and propagation. This paper examines the results related to a phase of the research activity, presently under course on such materials, aimed to study their fatigue behaviour.

---

[1] *Paper presented to "19° Convegno Nazionale AIAS", Pisa 15-16 Aprile, 1991.*

Materials examined

A microalloyed vanadium steel, 48MnV3 type, was employed. Its structural state results from a hot forging cycle on a 300 mm long and 90 mm square section bar, squeezed to half a length along a diagonal line until halving its size (induction heating, 4 to 5 minute heating time, 1060°C and 1240°C max temperature, 5 to 6 minute soaking, air cooling down to room temperature). Test pieces were obtained from an area not involved in deformation, in order to simulate the structural conditions of complex shape forged pieces in areas undergoing no or a very low deformation, and thus in the worst conditions of coarsened grain in lack of recrystallisation refining.

A comparison was made with a hardening and tempering steel, ASTM A533 B type, hardened and tempered at 600°C, which shows a homogeneous structure of tempered martensite, and exhibits a similar yield point level.

After simulation of the forging cycle at 1060°C, the microalloyed steel microstructure consists of proeuctectoid ferrite and pearlitic colonies together with free equiaxed grain ferrite. The ferrite is 34% in volume with an $HV_{15} = 182$ microhardness.

Pearlite shows an $HV_{15} = 224$ microhardeness. The pre-existing austenic grain dimensions are D = 48 to 52 μm (No. 5.5 on the ASTM scale). After simulation of the forging cycle at 1240°C, the microstructure is similar to the previous case, with a much coarser grain size. The pre-existing austenitic grain dimensions are D = 200 to 220 μm (No. 1 on the ASTM scale).

The HV_{15} microhardness is 139 for ferrite and 206 for pearlite. The reduced amount of proeuctectoid ferrite is due to the dropping of austenite transformation temperature the cooling during process, caused by the larger austenic size.

The chemical composition of the microalloyed steel is reported on Table 1, whilst Table 2 shows the mechanical characteristics of the steel employed.

TABLE 1 - Chemical composition of the microalloyed steel

C = 0.48%	Mn = 0.76%	Si = 0.23%	Ni = 0.11%	Cr = 0.11%	Mo = 0.02%
Cu = 0.23%	S = 0.030%	P = 0.013%	Al = 0.020%	V = 0.08%	

TABLE 2 - Mechanical characteristics

A533B	Hardened and tempered	Microalloyed T = 1060°C	Microalloyed T = 1240°C
R_m (MPa)	682	810	860
R_{el} (MPa)	566	508	520
E (MPa)	210.700	208.000	208.000
A (%)	21	17	10
Z (%)	80	21	8

Experimental testing

Test piece

Smooth cylindrical specimens were built with an 8 mm dia., as well as keyhole-type specimens with different fillet radii at the notch bottom end, in order to have different values of the theoretical over-stress concentration factor, K_t.

Tables 3 and 4 report the fillet radii, geometrical dimensions and corresponding K_t values for the materials under survey.

TABLE 3 - Geometric dimensions and K_t values for the hardened and tempered steel

Specimen	R (mm)	K_t	b (mm)	W (mm)	B (mm)
2R1	2	2.84	26.5	48.0	24.0
2R2	2	2.83	26.5	48.0	24.0
2Rp-1	2	2.68	20.0	36.0	17.0
2Rp-2	2	2.57	20.0	36.0	17.0
2Rp-3	2	2.50	20.0	36.0	17.0
4R-1	4	2.39	26.5	48.0	24.0
4R-2	4	2.40	26.5	48.0	24.0
4R-3	4	2.23	26.5	48.0	24.0
4R-4	4	2.20	26.5	48.0	24.0
12R-1	12	1.40	27.0	73.0	22.0
12R-2	12	1.46	27.0	73.0	22.0
12R-3	12	1.39	26.5	48.0	24.0

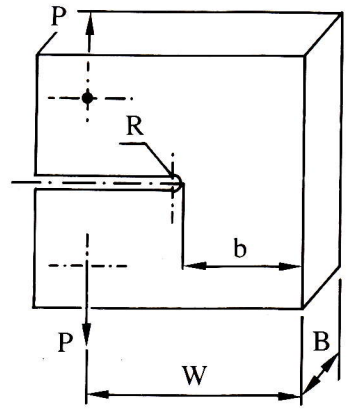

TABLE 4 - Geometric dimensions and K_t values for the microalloyed steel

	T = 1060 °C						T = 1240 °C				
Specimen	R(mm)	K_t	b(mm)	W(mm)	B(mm)	Specimen	R(mm)	K_t	b(mm)	W(mm)	B(mm)
2.5R-1	2.5	3.0	26.9	47.4	21.4	2R-1	2	3.0	27.0	48.0	24.0
2.5R-2	2.5	2.8	26.7	48.2	22.5	2R-2	2	2.9	"	"	"
2.5R-3	2.5	2.8	27.2	47.2	22.5	2R-3	2	3.2	"	"	"
4R-1	4	2.1	24.9	47.5	23.4	4R-1	4	2.2	"	"	"
4R-2	4	2.1	25.3	44.6	23.4	4R-2	4	2.1	"	"	"
4R-3	4	2.2	27.5	48.3	18.1	4R-3	4	2.1	"	"	"
12R-1	12	1.4	24.6	47.6	11.9	12-R1	12	1.7	"	"	"
12R-2	12	1.4	19.5	48.2	10.9	12-R2	12	—	—	—	—
12R-3	12	1.4	24.4	47.7	11.9	12-R3	12	1.4	"	"	"
						12R-3′	12	1.4	"	"	"

Fatigue tests

Two different types of fatigue tests were carried out. One of them on the smooth cylindrical

specimens where an alternating axial load was applied with tests under controlled deformation condition; and the other on notched specimens where a pulsating load between $P = \mathbf{0}$ and $P = P_{max}$ was applied, with tests under controlled load condition.

Deformations were measured by electrical strain gauges glued to the notch bottom end and to the keyhole-type specimens.

The nucleation phase in the smooth specimens is identified by a 10% decrease in the stress amplitude, σ_a (see Fig. 1). The tests on the notched specimens, instead, are interrupted when a crack is detected by the fluorescent penetrant method.

Experimental results

Smooth specimens

Figs. 2 and 3 show the amplitude of elastic, plastic and total strain, as defined in Fig. 1, in terms of the fracture or nucleation cycle numbers as derived from tests being performed on smooth specimens both from hardened and tempered steel and microalloyed steel, with a forging temperature of $t = 1240\,°C$.

The two materials display quite a different behaviour. In the area with prevailing plastic strains, it is the hardened and tempered steel that discloses a higher fatigue life, whereas on increasing cycle umbers towards a limitless fatigue life, the microalloyed steel is characterised by a higher elastic strain.

In Fig. 2 two different curves can be recognised for the hardened and tempered steel, one of them at the complete failure of the specimen and the other at crack nucleation, which is identified by a 10% decrease in the initial stress value.

In the case of microalloyed steel, instead, no nucleation phase was identified. In fact, hysteresis cycles stay virtually unchanged until the complete failure of the specimen.

In Fig. 4, the trends of the stress amplitude, σ_a, as a function of the cycle numbers are compared for two specimens, one of them from hardened and tempered steel and the other from microalloyed steel, whereon the same strain value, $\varepsilon_{a,t} = 10{,}000$ μm/m, was imposed.

In the case of the hardened and tempered steel, after the hysteresis cycle stabilisation, one can recognise the presence of a crack nucleation phase, corresponding to a decreased stress amplitude σ_a. On the contrary, no such phase is to be seen in the case of the microalloyed steel.

The different behaviour of the two materials is also evidenced (Fig. 5) by the cyclic curves expressed by the relation:

$$\sigma_a = K' \, (\varepsilon_{a,p}) \rightarrow {}^{n'} \qquad (1)$$

as well as by the higher strain hardening detected in the case of the microalloyed steel.

The microalloyed steel shows a far less tough behaviour. In fact, the fatigue crack nucleates at the pearlite interlamellar separation and is likely to propagate in an instable way.

The fracture area at the abrupt failure is characterised by cleavage separations, whereas in the hardened and tempered steel the failure is tough type with extended plastic deformation areas. Such a behaviour is shown in Fig. 6.

The more fragile behaviour of the microalloyed steel is shown in Fig. 7, which reports the relationship trends between the propagation area of the fatigue fracture and the total resistance area. It is worth noting that the crack propagation area in the microalloyed steel is less extended than in the hardened and tempered steel.

Notched specimens

The scope of the tests on these specimens is to evaluate the different fatigue behaviour of materials, in the presence of a notch.

The applied load values are enough for a plastic strain of the material at the notch bottom end, whilst in the remaining portion the material is still within the elastic range. After the first load cycle, the average stress is virtually null, as one can see from Fig. 8, and the subsequent test conditions prove to be similar to the imposed strain tests with medium-high strain degree, also because the heavily deformed area is of limited extension and constrained by the elastic behaviour of the surrounding material.

Therefore, in order to compare the fatigue life of both notched and smooth specimens, the value of the strain amplitude $\varepsilon_{a,t}$ as defined in Fig. 8 is considered.

The notch effect on the specimen fatigue life and behaviour is, as everybody knows, quite meaningful. In smooth specimens $K_t = 1$, the strain value is the same throughout the section and no collaboration is to be seen in the surrounding material. In notched specimens, instead, the presence of a strain and stress gradient entails a lower extension of the plastic deformed areas [3,4].

A relative stress gradient can be defined:

$$\chi_\sigma = (1/\sigma_{max})\ (d\sigma/dx)_{x=0} \qquad (2)$$

Within the proportional limit, defining a strain gradient is equivalent:

$$\chi_\varepsilon = (1/\varepsilon_{max})\ (d\varepsilon/dx)_{x=0} \qquad (3)$$

Tables 5 and 6 report the gradient values, calculated within the proportional limit, considering $d_x = \Delta_x = 1$ mm, for the hardened and tempered steel and microalloyed steels, respectively.

If the proportional limit is exceeded, then it seems more meaningful to consider a deformation gradient χ_ε, which is no longer directly correlated to the stress gradient.

The loads applied to notched specimens are such as to overcome the yield load in the most stressed area at the notch bottom end. That is why a relative stress gradient was calculated at the third load cycle, considering the actual trend of the total strains on the specimen faces, obtained through strain-gauge measurements. Thus Tables 5 and 6 report the values so calculated, that is, keeping account of the total strain variation, $\varepsilon_t = \varepsilon_m + \varepsilon_{a,t}$, divided by the strain amplitude value, $\varepsilon_{a,t}$. The same tables also report the fatigue life values of notched specimens, experimentally measured at the crack nucleation.

From an analysis of the values measured on hardened and tempered specimens (Table 5), a link appears between gradients χ_ε and specimen fatigue life, where one can see that, the load level being the same, fatigue life N_f will vary with the changing gradient. Further, as for the specimen groups with the same fillet radius, the gradient will vary gradually and steadily with the changing load level.

From Tables 5 and 6, instead, one can note a certain scattering of the experimental data related to the strain gradient duration and value, thus disclosing a rather random behaviour at the crack nucleation due to the peculiar microstructure of the material. The specimens built from microalloyed steel forged at t = 1060°C, generally show a tougher and more homogeneous fatigue behaviour than the steel

forged at t = 1240°C. The values of the elastic and total strains, measured during fatigue tests and constant cycle intervals through electric strain gauges glued to the specimens, show that steels after low temperature forging display higher plastic strain values than the other steel [5,6].

TABLE 5 - Strain gradients for specimens in hardened and tempered steel

Specimen	K_tS(MPa)	$\chi_{\varepsilon el.}$	χ_ε	N_f
2R-1	1050	0.66	0.76	70000
2R-2	1120	—	—	50250
2Rp-1	1050	0.64	0.75	85000
2Rp-2	1120	0.64	0.73	53000
2Rp-3	1200	0.63	0.86	24500
4R-1	1050	—	—	61000
4R-2	1120	0.38	0.44	27000
4R-3	1200	—	—	13000
4R-4	1260	0.40	—	14600
12R-1	1050	0.27	0.39	22000
12R-2	1120	0.26	0.50	20000
12R-3	1200	0.26	0.52	10000

TABLE 6 - Strain gradients for specimens in microalloyed steel

	T = 1060°C					T = 1240°C			
Specimen	K_tS(MPa)	$\chi_{\varepsilon el.}$	χ_ε	N_f	Specimen	K_tS(MPa)	$\chi_{\varepsilon el.}$	χ_ε	N_f
2.5R-1	1050	0.46	0.54	61500*	2R-1	1050	0.48	0.61	67000
2.5R-2	1120	0.43	0.68	28000	2R-2	1120	0.47	0.68	34000
2.5R-3	1200	0.44	0.62	20000	2R-3	1200	0.49	0.66	29000
4R-1	1050	0.38	0.48	27000	4R-1	1050	0.38	—	29000
4R-2	1120	0.36	0.54	25000	4R-2	1120	0.41	0.54	21500*
4R-3	1200	0.38	0.55	—	4R-3	1200	0.37	0.52	20000*
12R-1	1050	0.22	0.32	27300*	12R-1	1050	0.21	0.36	39000
12R-2	1120	0.24	0.77	—	12R-2	1120	—	—	—
12R-3	1200	0.19	0.58	8000	12R-3	1200	0.21	0.37	—
					12R-3′	1200	0.20	0.19	—

* Instable propagation of the crack

The predictions for the fatigue life of notched pieces through the use of the Manson-Coffin law in the case of the hardened and tempered steel, are always to be considered as very conservative.

In fact, when considering, for instance, the specimen 2R-2 of Table 5 and thus with a high gradient, the Manson-Coffin calculated value proves to be $N_{f,t} = 16{,}050$ with a ratio $N_{f,t}/N_f = 0{,}32$, as against a fatigue life of $N_f = 50{,}250$ found out on an experimentally basis. On the contrary, as regards the specimen 12R-1, with a lower gradient, the difference between the predicted value $N_{f,t}$ and the experimental one N_f will decrease. In fact, $N_f = 22{,}000$ and $N_{f,t} = 15{,}380$, with a ratio $N_{f,t}/N_f = 0.70$.

As for the microalloyed steel forged at t = 1240°C, the equivalent specimen 2R-2 of Table 6 gives

$N_f = 34{,}000$ and $N_{f,t} = 31{,}739$ with a ratio $N_{f,t}/N_f = 0.93$, whereas for the specimen 12R-1 we will find $N_f = 39{,}000$ and $N_{f,t} = 37{,}354$ with a ratio $N_{f,t}/N_f = 0.96$.

From the above, one can infer that, in the case of the hardening and tempering steel, the notched specimen strength will notably improve with increasing gradient owing to the collaboration of the surrounding material. One the contrary, the microalloyed steel will stay virtually impervious to the gradient effect due to its low toughness value.

Conclusion

The tests carried out on smooth specimens according to Manson-Coffin methodology show that the microalloyed steel, as compared to the hardening and tempering steel, displays a higher strength in the elastic range, whereas in the case of large plastic deformations the hardening and tempering steel shows a better behaviour.

In the presence of either notches or a stress and strain gradient, the microalloyed steel proves to be significantly insensitive to their variations, differently from what occurs in the hardened and tempered steel.

The behaviour actually investigated shows that crack appearance in microalloyed steels, occurs abruptly and with no appreciable plastic strain, whereas in hardening and tempering steel a gradual increase is to be seen in the total deformation during the nucleation period. That is to be traced back to the mixed structure with a high percentage of lamellar pearlite in the microalloyed steel. Such a structure, in fact, is less suited to withstand the fatigue crack nucleation than the homogeneous structure of tempered martensite in the hardened and tempered steel.

Acknowledgements

This work was supported by a M.U.R.S.T. GRANT.

References

[1] D.J. Naylor, *Review of international activity on microalloyed engineering steels*, Ironmaking and Steelmaking, Vol. 16, 1989, N. 4, 246-252.

[2] S. Engineer, B. Huchtemann, W. Schueler, *A review of the development and application of microalloyed medium carbon steels*, Steel Research, Vol. 58, N. 8, 369-376.

[3] G. Glinka, *Calculation of inelastic notch-tip strain-stress histories under cyclic loading*, Eng. Fracture Mech., 1985, Vol. 22, N. 5, 839-854.

[4] S. Schijve, *Stress gradients around notches*, Fat. of Eng. Mat. and Structures, 1980, Vol. 3, N. 4, 325-338.

[5] M. Balbi, M. Boniardi, M. Giglio, L. Vergani, *Comportamento a fatica di acciai microlegati a medio tenore di carbonio*, La Meccanica Italiana, 1990, N. 242, 42-49.

[6] L. Vergani, M. Giglio, M. Balbi, G. Silva, *Nucleation of fatigue cracks in microalloyed forging steel, Evolution of Advanced Materials*, AIM-ASM (Europe) International Conference, Milano, 1989.

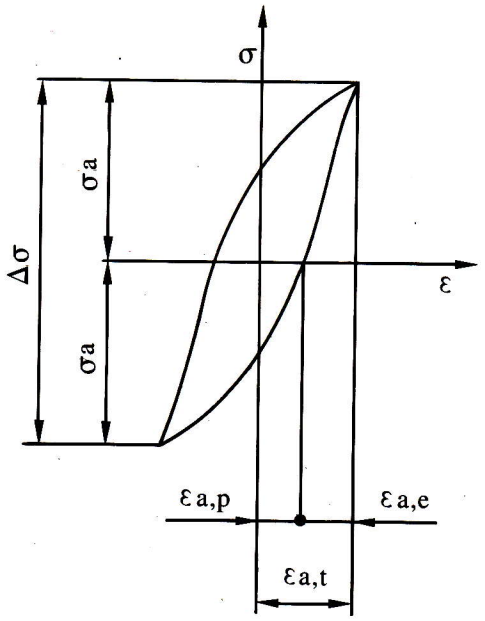

Fig. 1:
Definition of the hysteresis cycle parameters.

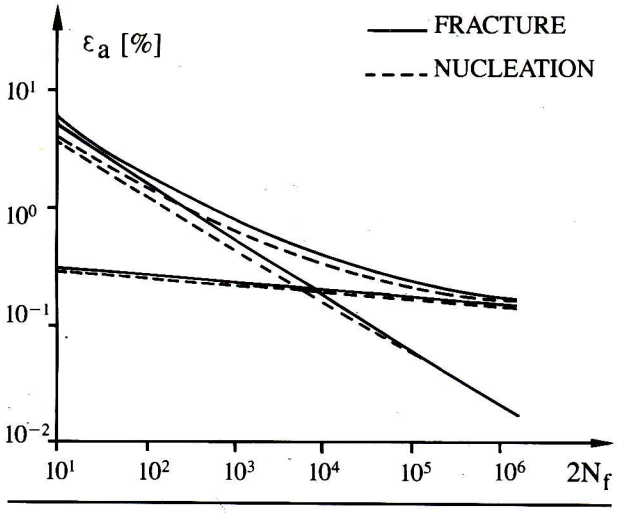

Fig. 2:
Curves $\varepsilon - N_f$ for the hardened and tempered steel.

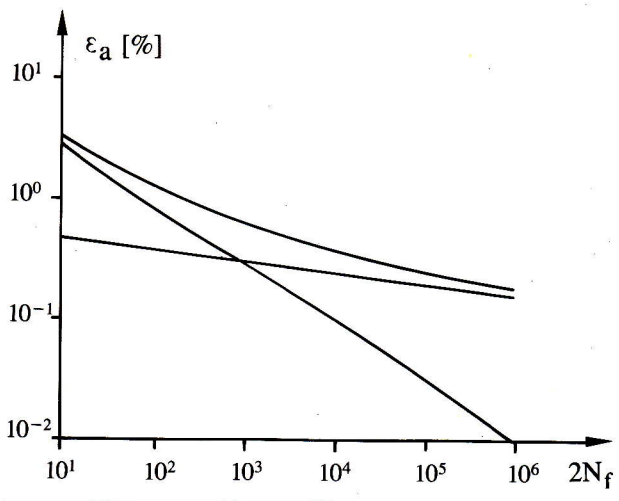

Fig. 3:
Curves $\varepsilon - N_f$ for the microalloyed steel.

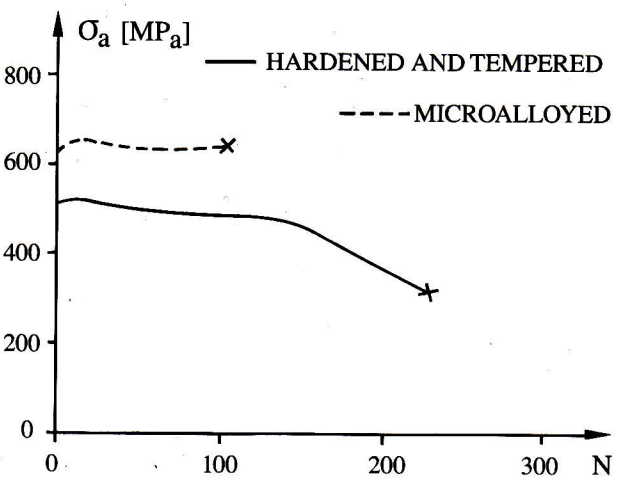

Fig. 4:
Curve $\sigma_a - N$ for smooth specimens with equal $\varepsilon_{a,t}$ imposed.

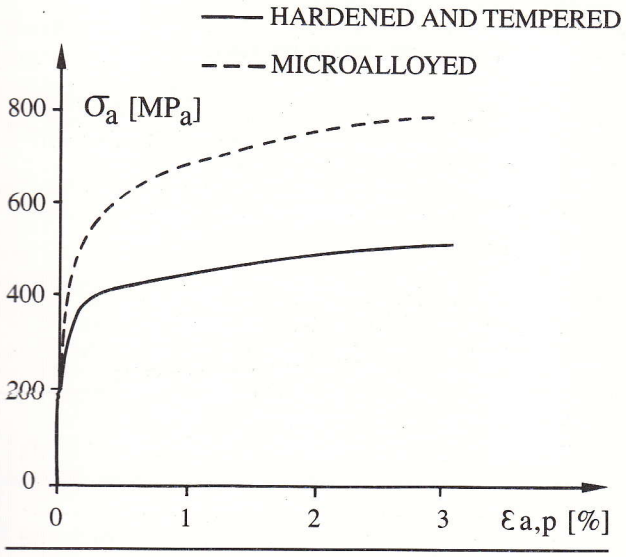

Fig. 5:
Cyclic curves $\sigma_a - \varepsilon_{a,p}$.

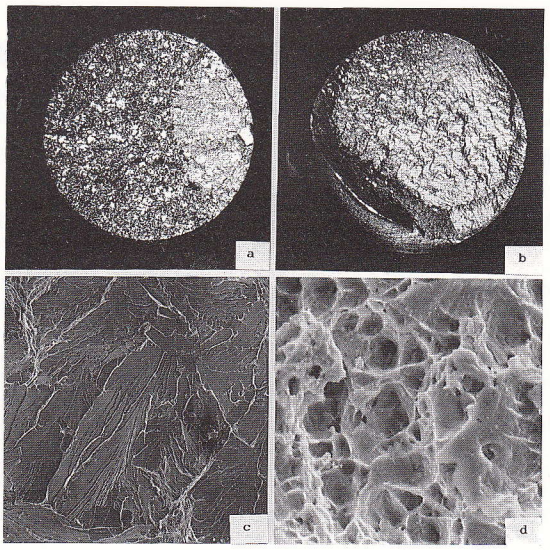

Fig. 6:
View of fracture areas in the materials under investigation:
a) microalloyed steel 48MnV7 (test $\varepsilon - N, \varepsilon_{a,t} = 4{,}190$ μm/m, $N_f = 3{,}633$), X8
b) hardening and tempering steel A533B (test $\varepsilon - N, \varepsilon_{a,t} = 5{,}000$ μm/m, $N_f = 2{,}509$), X8
c) details of the abrupt fracture area for the microalloyed steel, X300
d) details of the abrupt fracture area for the hardening and tempering steel, X10,000

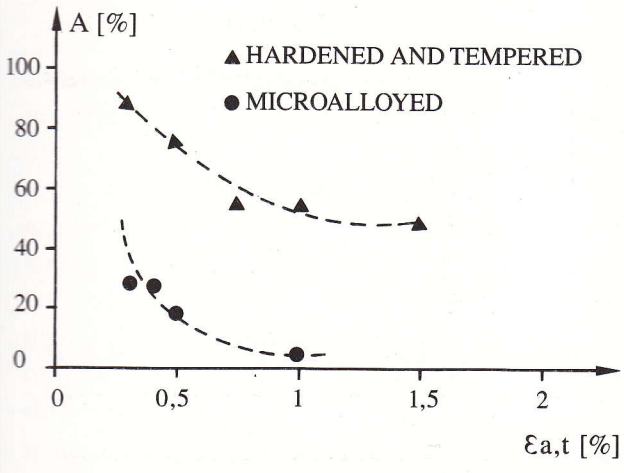

Fig. 7:
Percent propagation areas for smooth specimens.

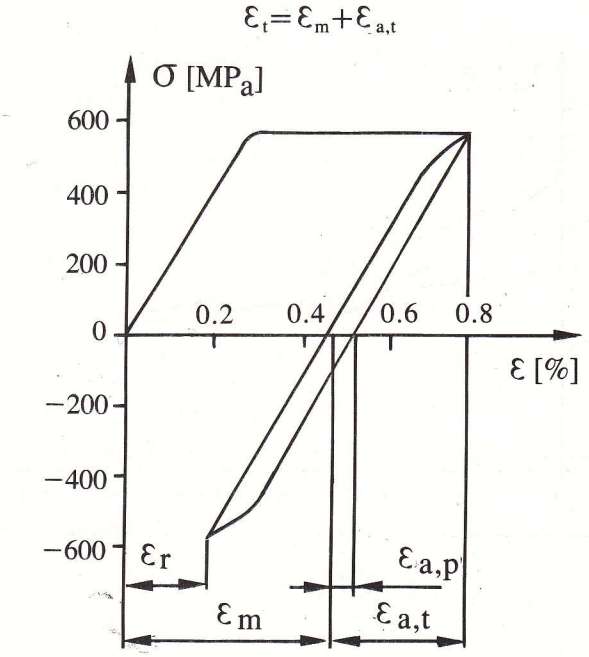

Fig. 8:
Strain cycle parameters at the first load cycle.